TMI-2 LOWER VESSEL DEBRIS EXAMINATIONS[a]

Douglas W. Akers and Charles S. Olsen
Idaho National Engineering Laboratory
EG&G Idaho, Inc., P.O. Box 1625,
Idaho Falls, Idaho 83415
(208) 526-4064 and (208) 526-9094

and

R. V. Strain
Argonne National Laboratory
Argonne, Illinois

ABSTRACT

Samples of prior molten debris have been retrieved from the lower reactor head of the TMI-2 reactor. Preliminary results of the examination of these samples are presented with particular emphasis on the metallurgical and radiochemical characteristics of the materials. Areas of nearly pure fuel material in a stoichiometric, $(U,Zr)O_2$ matrix occurred which indicate temperatures approaching the melting point of UO_2 (up to 3100 K). Comparison of the measured radionuclide concentrations in the debris with ORIGEN-2 calculated concentrations indicates significant retention of Cs-137 (up to 22%) in the prior molten debris. Autoradiography results suggest significant accumulations of activity on the surfaces of voids in the debris and at grain boundaries.

INTRODUCTION

The Unit 2 pressurized water reactor at Three Mile Island (TMI-2) underwent a loss-of-coolant accident on March 28, 1979, resulting in severe damage to the reactor core. After the accident, four organizations, General Public Utilities Nuclear Corporation (GPU Nuclear), Electric Power Research Institute (EPRI), the Nuclear Regulatory Commission (NRC) and the Department of Energy (DOE), collectively known as GEND, began a postaccident evaluation of the TMI-2 accident. Acquisition of the data is important as TMI-2 is the only example of a full scale loss-of-coolant accident. As part of this evaluation, samples of debris were removed from the lower head of the reactor vessel (Figure 1).

---

[a]Work supported by the U.S. Department of Energy, Assistant Secretary for Nuclear Energy, Office of Light Water Reactor Safety and Technology, under DOE contract No. DE-AC07-76-ID01570.

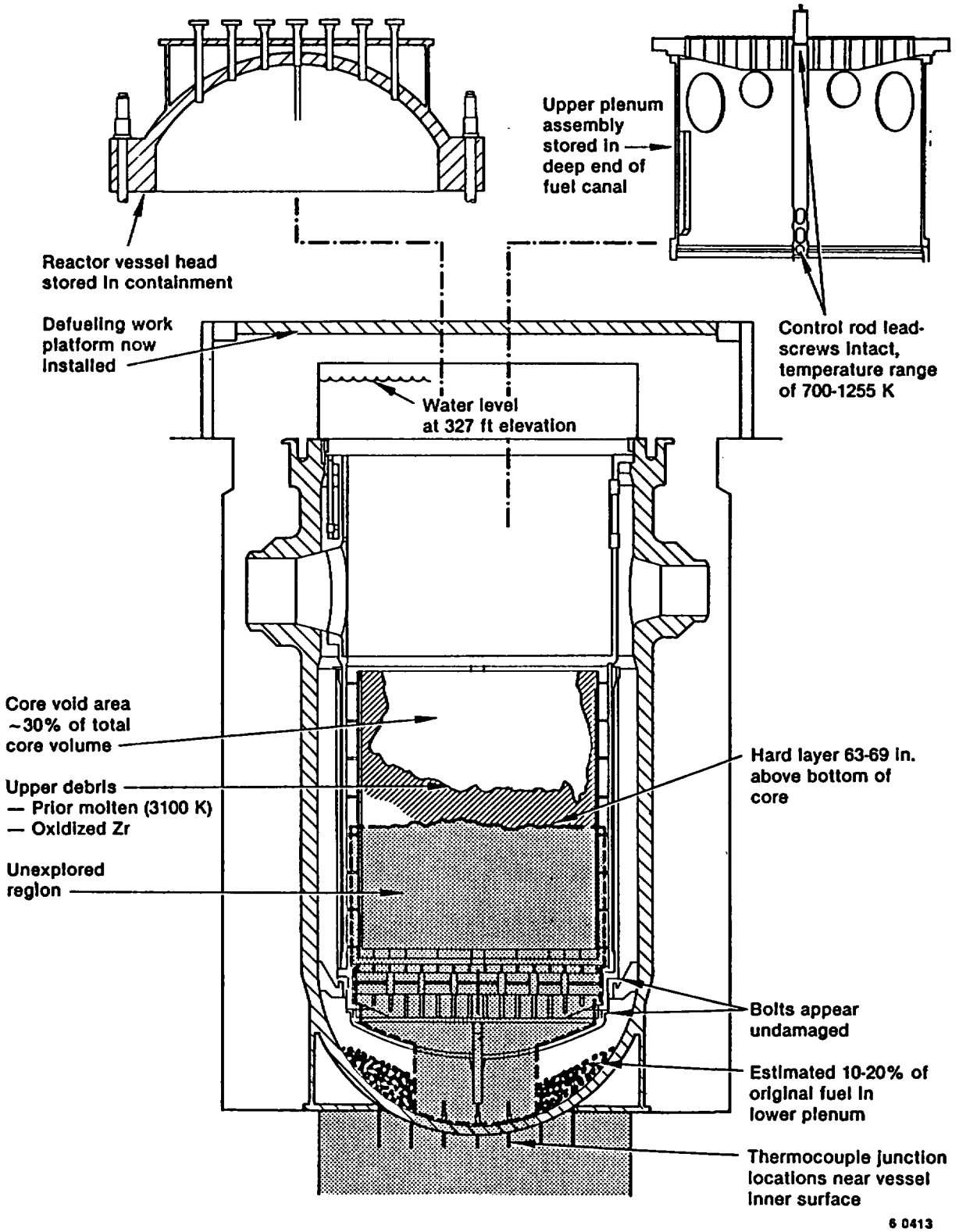

Figure 1. Known current condition of TMI-2 core.

The objective of this paper is to present results of the examination of samples obtained from the lower head of the reactor vessel and to address some of the mechanisms that may account for the observed behavior.

The lower vessel debris samples were obtained through the 25-cm annulus between the thermal shield and the reactor vessel that provides access from the top of the reactor vessel to the lower reactor vessel cavity. The samples were removed using a jointed, long handled tool (>4 m in length) to grab samples of debris at various locations on the lower reactor vessel head. All samples removed from the lower vessel debris bed were removed from inspection ports No. 7 and 11 on the south and southwest sides of the core. Based upon video inspections of the lower vessel cavity, 10% to 20% of the original core mass (up to 20,000 kg) is estimated to have been relocated to the lower reactor vessel head. Eleven samples were removed from the debris bed; seven pieces ranging in size from 1-cm to 6-cm diameter were selected for examination.

A series of physical, metallurgical, and radiochemical examinations were performed on the debris samples. The physical characterization measurements included both material properties and mechanical behavior tests. The physical measurements included porosity, dry weight, immersion density, and associated radiation field. Mechanical properties measurements, e.g., drilling properties and crushability, were performed to support the reactor defueling effort now being performed by GPU Nuclear. The metallurgical examinations were performed to characterize the full range of metallurgical properties of the debris (e.g., grain size, composition, oxygen content, etc). Analyses were performed using optical metallography, scanning electron microscopy with energy dispersive x-ray analysis, Auger electron spectroscopy, microprobe analysis, and x-ray diffraction analysis. The radiochemical measurements were made to determine the chemical composition of the debris and to define the extent of radionuclide retention in the debris. Measurement techniques used included gamma spectroscopy, neutron activation analysis, liquid scintillation analysis, and delayed neutron production.

Although a brief discussion of the physical property tests is presented, the principal focus of this paper is the metallurgical and radiochemical characteristics of the prior molten debris relocated to the reactor vessel lower head. In addition, a brief discussion is presented of the current understanding of radionuclide behavior in the upper debris bed above the consolidated core portion as related to the lower vessel debris results.

PHYSICAL PROPERTIES OF LOWER VESSEL DEBRIS

Physical property measurements were made on the debris from the lower reactor vessel head to generally characterize the size of the material, radiation field, dry weight, immersion density, and open porosity. Table 1 lists the results of these measurements for the eleven particles recovered from the lower reactor vessel. The measurement of most importance for analysis purposes is the matrix density of the material which ranges from 6.6 to 8.1 g/cm^3. This is 23 to 37% less than the density of intact fuel material ($\sim$10.5 g/cm^3). The

TABLE 1. PHYSICAL PROPERTIES OF LOWER VESSEL DEBRIS

Particle Number	Size (Inches)	Radiation Measurements[a] Beta/Gamma (R/hr)	Gamma (R/hr)	Dry Weight W d (g)	Envelope Density (g/cc)	Open Porosity (%)
7-1	1.2 x 1.0 x 0.8	13	1.6	50.1	6.57	0.0
7-6	0.4 x 0.2 x 0.2	1.2	0.13	1.0	--[b]	--[b]
7-7	0.2 x 0.2 x 0.1	0.8	0.10	0.4	--[b]	--[b]
11-1	1.5 x 0.7 x 0.6	12	1.2	39.7	8.08	2.0
11-2	1.8 x 1.3 x 1.2	26	3.0	123.9	6.79	2.75
11-4	1.8 x 1.0 x 1.0	25	2.9	107.1	6.72	3.14
11-5	2.5 x 2.5 x 2.2	>50 42[c]	7.5 5.5[c]	553.9	6.47	1.99
11-6	0.7 x 0.7 x 0.4	4	0.5	12.7	6.3	5.0
11-7	1.6 x 1.2 x 1.1	30	3.2	118.8	7.09	1.20
11-10	0.4 x 0.2 x 0.2	0.7	0.1	0.6	--[b]	--[b]
11-11	0.5 x 0.5 x 0.5	3.5	0.32	5.5	--[b]	--[b]

a. Radiation readings were taken at rear of ARA Hot Cell. Background readings were 80 mR/hr β/γ and 50 mR/hr γ at 8 in.

b. Due to relatively small particle size and sensitivity limits of triple beam balance used to weigh particles, saturated and immersion weights could not be made.

c. Reading taken at 10 inches. At 8 inches, detector was off scale (>50 R/h β/γ).

reduction in density is probably due to several factors, including: (a) apparent voids present in the material, (b) presence of less dense, oxidized zirconium in the debris, and (c) granular structure of the debris.

The other physical tests performed on the debris were mechanical property tests to evaluate different types of drilling tools that could be used on the debris and to determine the compressibility of the debris. The results of these analyses will be presented in the final report on the lower vessel debris examinations.

METALLURGICAL PROPERTIES OF LOWER VESSEL DEBRIS

The general appearance of the sections showed the samples consisted of a continuous matrix with a number of large voids representing 25 to 40% of the sample surface (Figure 2). At a few locations, the porosity was only a few percent. The particle material was essentially all ceramic with a relatively small amount of metallic inclusions.

Electron microprobe data show the matrix materials were composed of 66.9 wt % U, 15.6 wt % Zr, 0.9 wt % Fe, 0.4 wt % Cr, 0.3 wt % Si, and

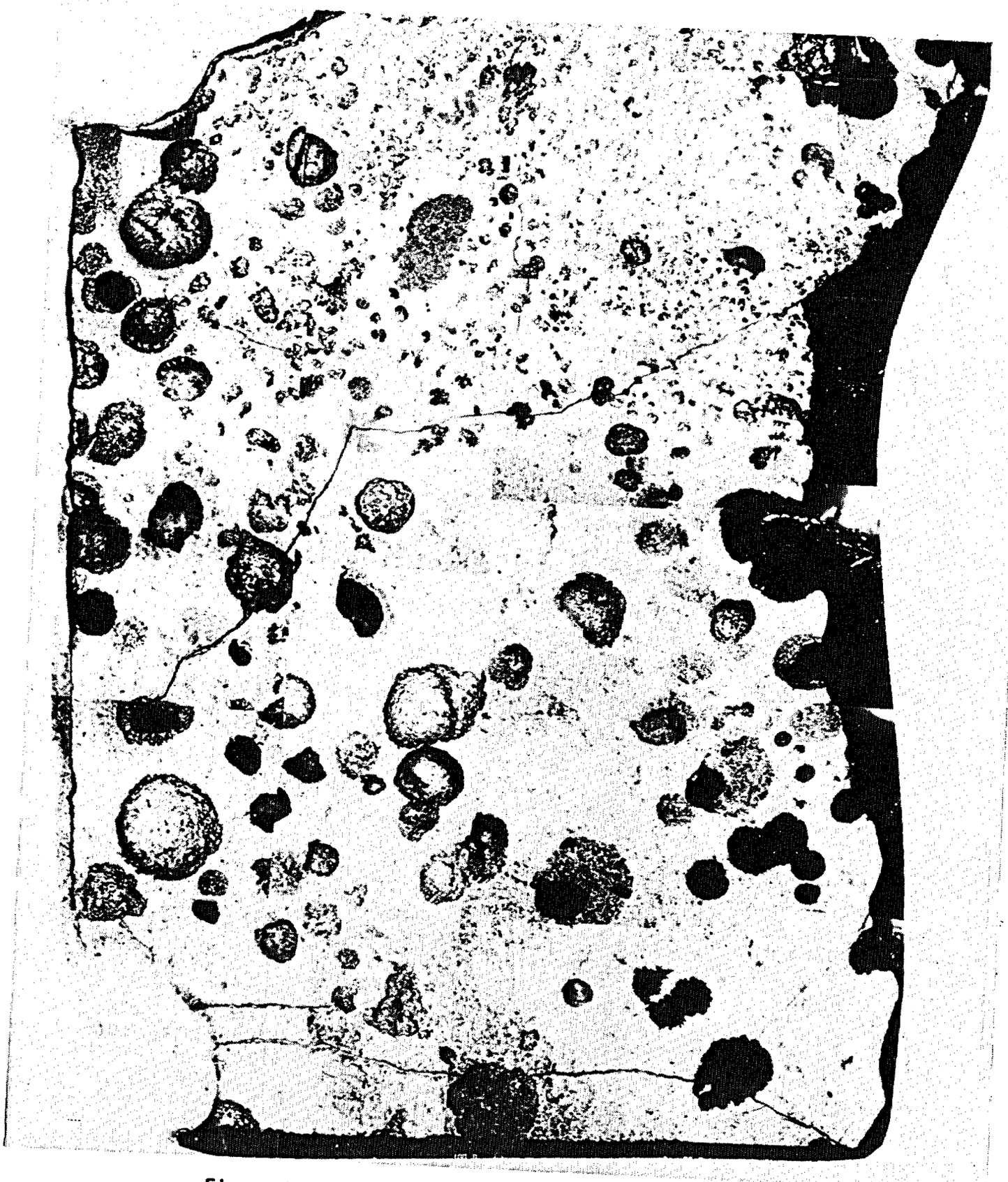

Figure 2. Porosity in cross section of particle.

0.1 wt % Ni. In this analysis, the undetected material is all assumed to be oxygen. Assuming all these elements are stoichiometric oxides, then, the equivalent composition is 75.9 wt % UO_2, 21.1 wt % ZrO_2, 1.8 wt % FeO, 0.6 wt % Cr_2O_3, 0.7 wt % SiO_2, and 0.2 wt % NiO.

The grain boundaries were generally found to be broad and exhibited a dendritic structure as shown in scanning electron microscopy (SEM) photographs (Figures 3 and 4). The dark phase in the grain boundaries of all samples examined was found to contain Fe and Cr along with variable amounts of Al and Ni (Figure 4). The dark phase was comprised primarily of Cr and Fe with detectable amounts of Al, Ni, and U.

Electron microprobe data for the grain boundary phase, which apparently contained Al and Ni, showed relatively high concentrations of Cr and Fe and higher concentrations of Ni than the matrix. Assuming the elements to be oxides, a material balance still could not be achieved, and because the electron microprobe was not capable of detecting Al, the deficiency is assumed to be aluminum. The light spots in the grain boundaries represent a high atomic number and is assumed to be UO_2. If the detected elements are assumed to be oxides and the undetected material is Al_2O_3, a relatively high concentration of Al will be present. On this basis, with the U and Zr assumed to be from the matrix, the average composition of the dark phase in the grain boundary will be 26.9 wt % FeO, 28.1 wt % Cr_2O_3, 38.7 wt % Al_2O_3, 4.8 wt % NiO, and 2.0 wt % SiO_2. The Si content in the dark phase of the grain boundary is about the same as the matrix.

An effort was made to locate and determine the composition of any metal inclusions present in the pores. Two small particles identified by energy dispersive spectroscopy (EDS) as silver appeared to be spongy at high magnification. The examination of several other voids considered to possibly contain metal particles did not produce additional metallic material. A small particle, dissimilar to the sample matrix, was found in a large crack. From EDS analysis, the material was determined to be primarily Zr, but also contained Fe and Cr, and appeared to be fully oxidized as it did not appear metallic during optical microscopy.

In the largest particle extracted from the lower plenum, small areas were found in which a second or intermediate phase surrounded the primary grain boundary. Most samples did not have a secondary phase surrounding the grains. Only U and Zr were present in this phase, and the U/Zr ratio was the same as for the matrix phase. Electron microprobe analysis indicated the composition of this intermediate phase was similar to the matrix phase. The average composition from two measurements on this phase indicated it contained 74.9 wt % UO_2, 19.5 wt % ZrO_2, 1.3 wt % FeO, 0.7 wt % Cr_2O_3, 1.0 wt % SiO_2, and 0.2 wt % NiO. The stoichiometry of these compounds is assumed since the microprobe is unable to detect oxygen. These data indicate the intermediate phase may be slightly lower in Zr than the matrix and may contain undetected elements (low atomic number) because the sum of the elements detected was 97.8 wt %. For example, the Fe may be in the chemical form of Fe_2O_3 which would add more oxygen to the analysis.

In the largest particle extracted from the lower plenum, a UO_2 phase containing no zirconium was found (Figure 5). The interface between the

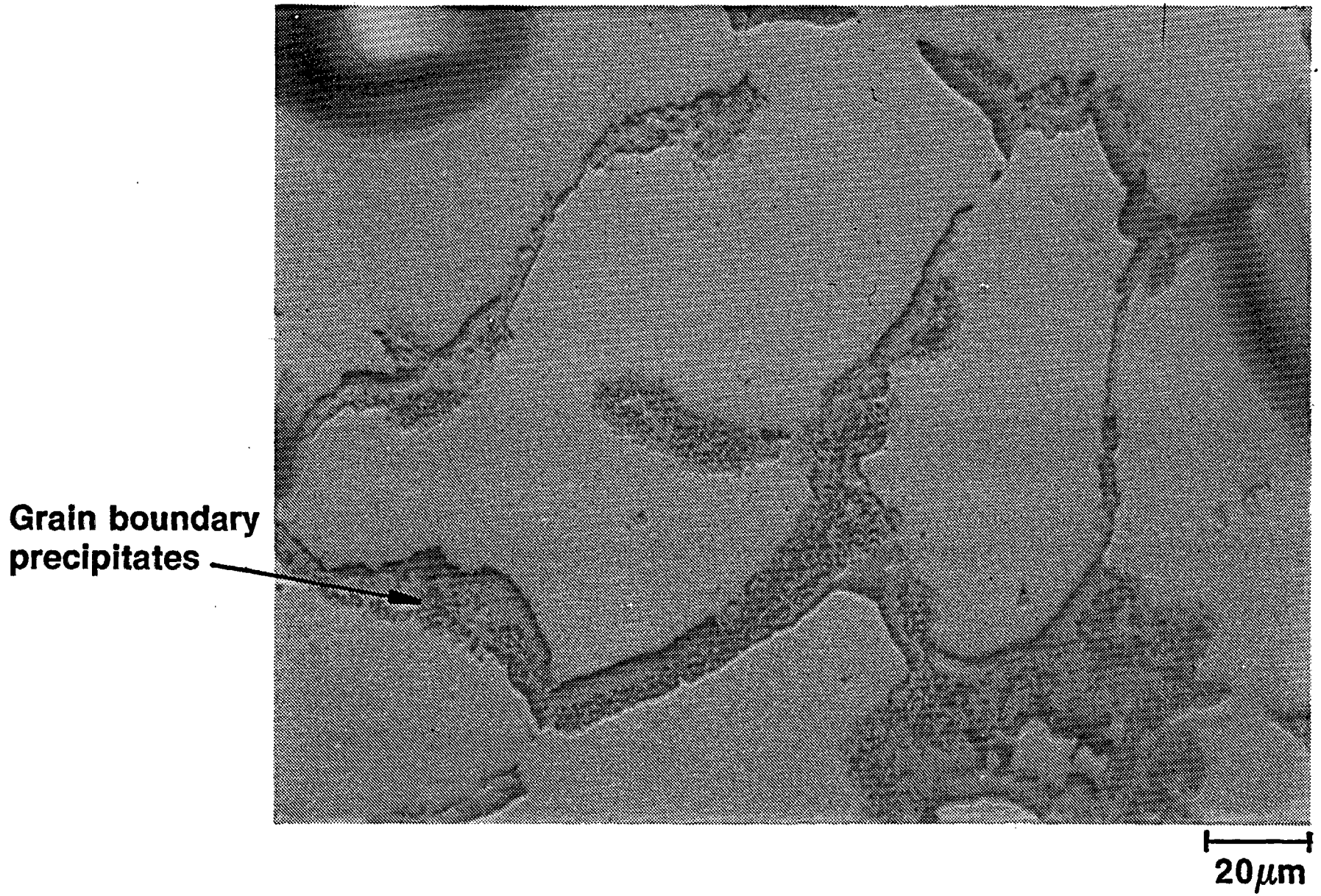

Figure 3. Grain boundary structure.

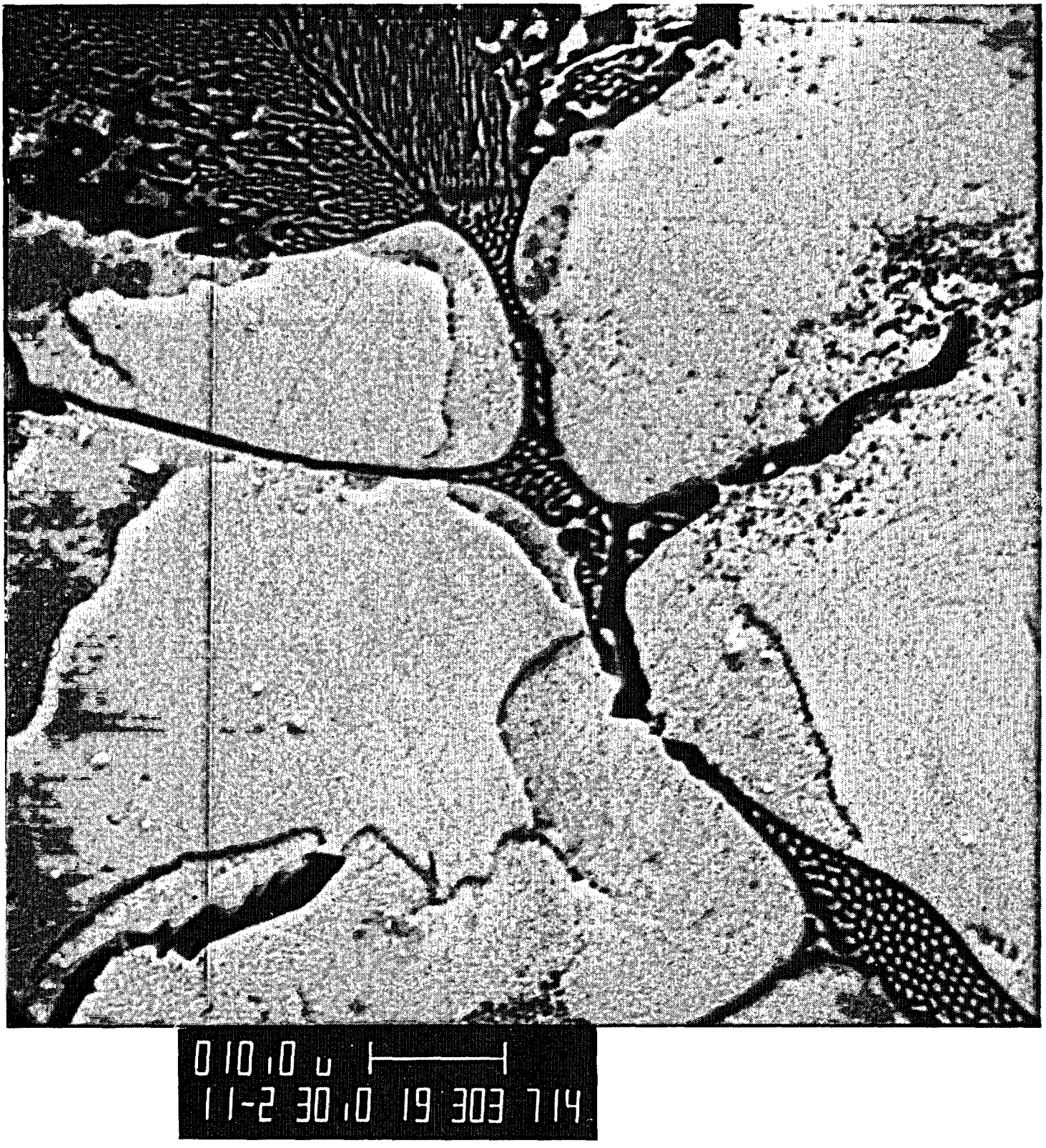

Figure 4. Dendritic structures in grain boundaries.

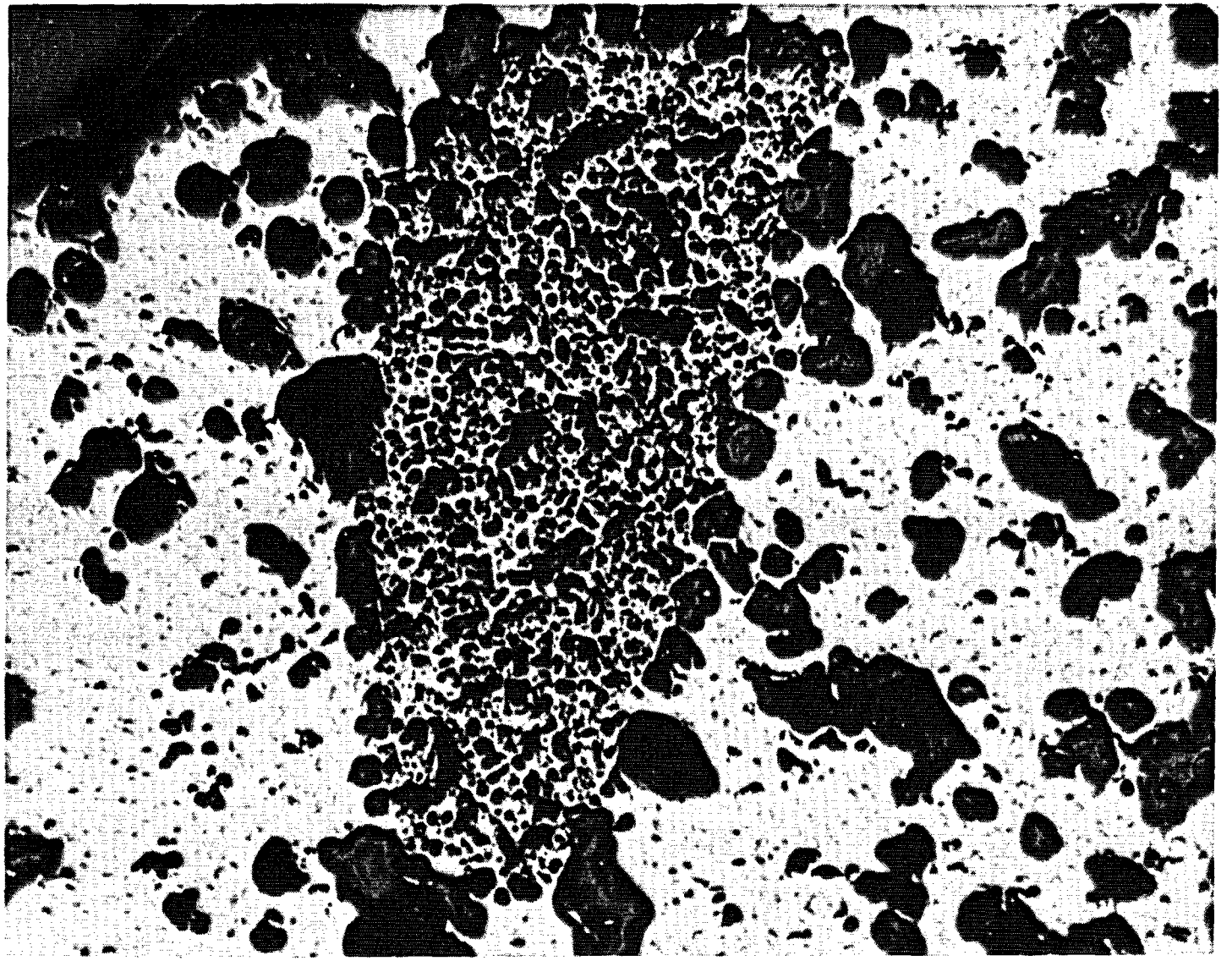

Figure 5. Pure UO_2 in U/Zr matrix.

pure UO_2 and the matrix consisting of uranium and zirconium dioxides is shown in Figure 6. The morphology of the porosity has changed compared with irradiated fuel at normal operating temperatures, but the grain size is still relatively small.

The detection limit for most elements on the SEM and the Auger is between 0.5 and 5 wt % under ideal conditions. Because this sample is radioactive, the signal to noise ratio is adversely influenced, particularly for the SEM. Therefore, elements in the sample with concentrations of less than 1 to 2 wt % were not detected by this analysis.

The general appearance of the lower plenum debris and the microstructure of the sample indicate it was once molten. The pure UO_2 inclusion in the largest particle may not have melted, but the change in porosity indicates it was near the melting point. This conclusion is consistent with the temperature of the matrix being about 3100 K (the liquidus temperature). The matrix of the sample consisted of materials present in large quantities as the fuel (UO_2) and the cladding. The Fe and Cr present in the grain boundaries and in the sample surface layer were present as constituents of stainless steel and inconel. The relatively high concentrations of Al in the grain boundaries may have come from Al_2O_3 in the form of insulating pellets in thermocouple and instrument leads and from the Al_2O_3/B_4C control rods.

The microstructure indicates the debris was cooled from a melt. The higher melting UO_2-ZrO_2 solidified first, and then the lower melting structural material oxides (Fe, Cr, and Al) solidified at a lower temperature.

RADIOCHEMICAL ANALYSIS RESULTS FROM LOWER VESSEL DEBRIS

Figure 1 shows the currently known damage state of the reactor core and the reactor vessel internals as determined from video characterizations and sampling and analysis of materials taken from the core.[1] The samples removed from the lower reactor vessel head were sectioned, and comparable sections were prepared for metallurgical and radiochemical analysis. Figure 7 shows the cross section of a particle used for the lower vessel debris analysis (Particle 11-5-C). This sample is 6-cm diameter at the longest dimension. The numbered locations are the points where sample material was removed for analysis. A principal feature of this sample is the varying porosity of the material. The porosity is generally greater at the top of the figure and lower at the bottom. The porosity estimates of the debris range from >25% at some locations to <2% at other locations.

One of the initial analyses performed was an autoradiographic analysis of the debris section shown in Figure 2. The autoradiograph of Particle 11-4-C is shown in Figure 8. The light areas indicate higher gross radiation areas, and the darker areas indicate zones of lesser activity. The high activity regions correspond with the void regions in Particle 11-4-C. These data indicate significant accumulations of activity on the void surfaces as evidenced by the circular high activity

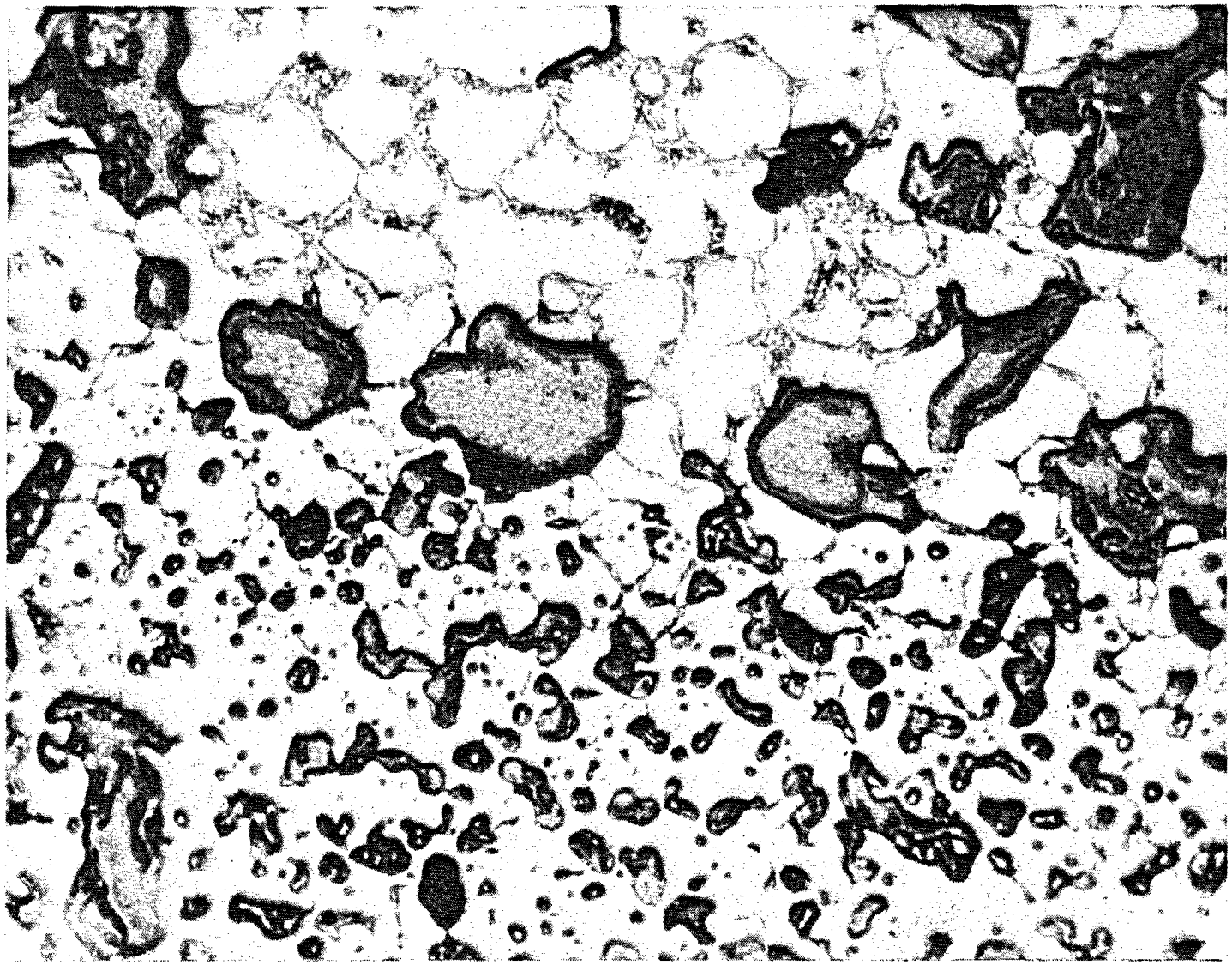

Figure 6. $UO_2/(U,Zr)O_2$ Interface (200X).

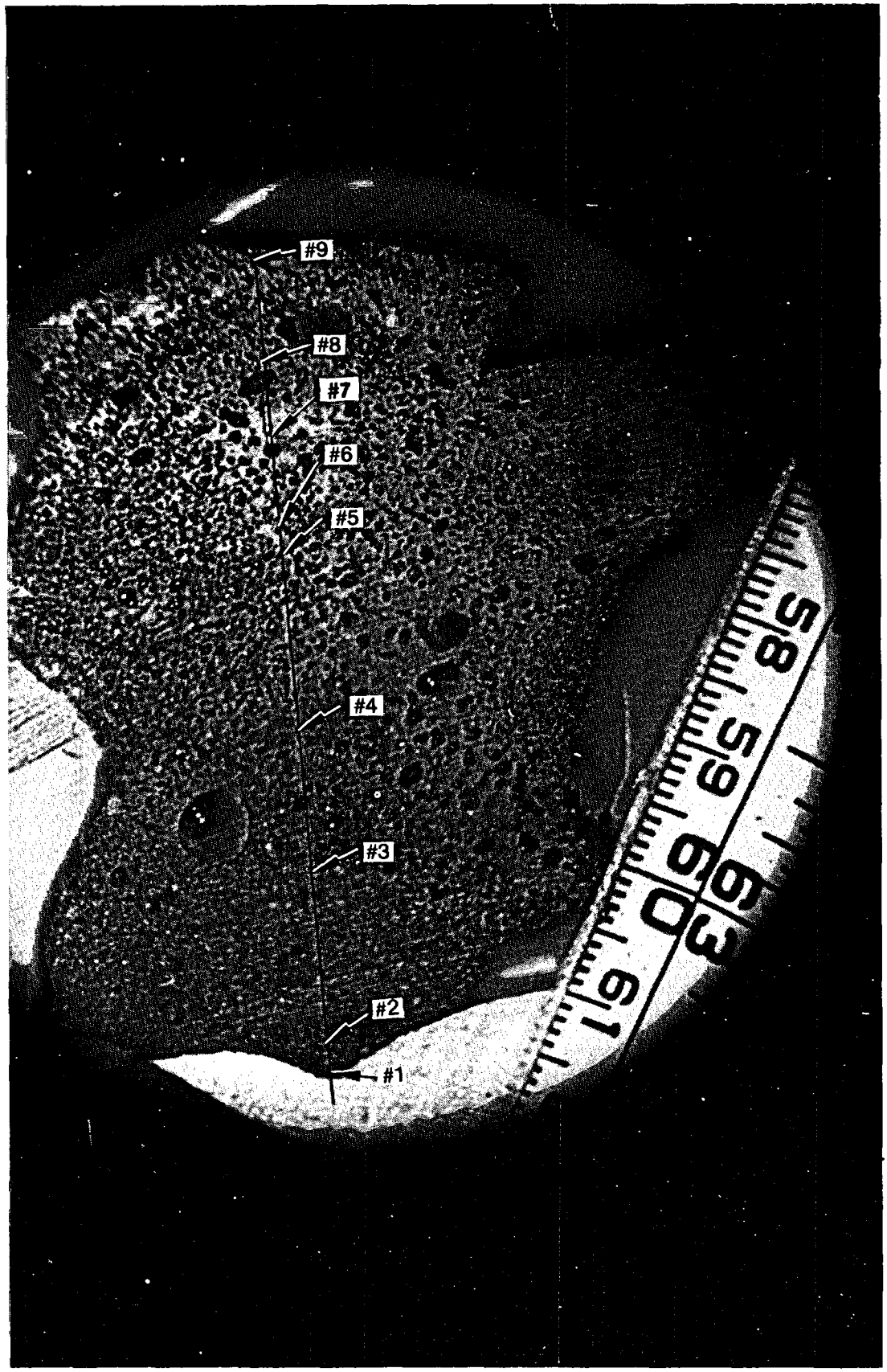

Figure 7. Particle 11-5-C radiochemical analysis locations.

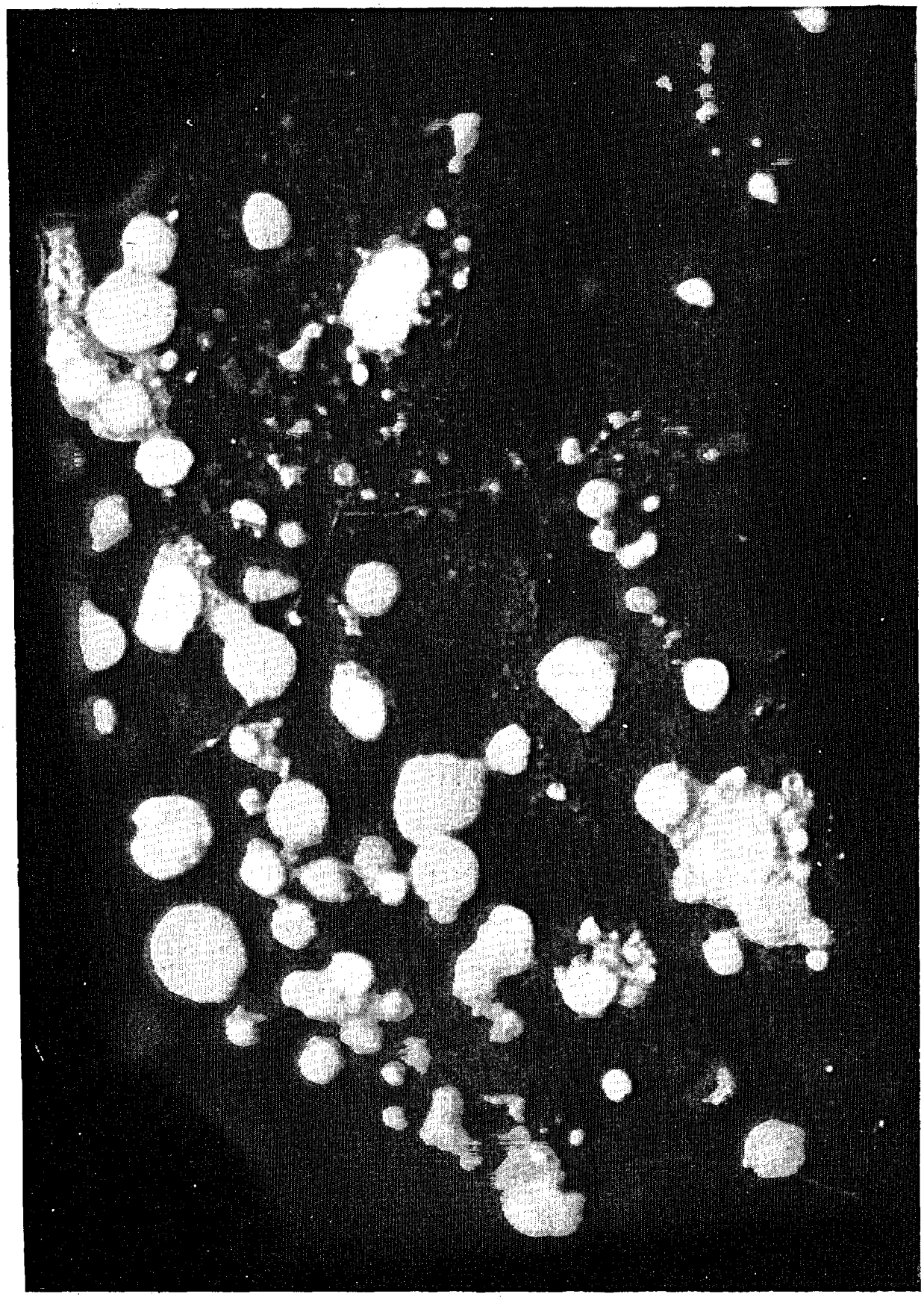

Figure 8. High fission product activity in voids of Particle 11-4-C.

regions. The radionuclide most likely deposited on these surfaces is Cs-137 which is one of the most active gamma ray emitters measurable in the debris. Closer examination of the autoradiographs also indicates accumulations of activity at the grain boundaries. Further analyses are being performed to determine the identity of the radionuclides deposited in the voids and at grain boundaries.

Elemental analyses were performed on the samples removed from Particle 11-5-C to determine if gross compositional variations could account for the differing porosity. The preliminary evaluation of these results indicates no apparent correlation between composition and porosity. Table 2 lists a comparison between the average measured elemental composition of Particle 11-5-C and the expected composition if the core structural materials were evenly mixed in the debris. The measured concentrations of uranium and zirconium are 12% and 41% less than expected, respectively. This difference is probably due to uncertainties in the analysis (~15%) and to oxidation of the structural materials and the zirconium cladding. A further comparison of the uranium content of the samples is shown in Table 3 which lists the average uranium content of all samples. These data are similar to the average expected concentration and suggest Particle 11-5-C is typical of the debris concentrations. Note the samples removed represent a small portion of the core (<0.001%) and may not be representative of all debris transported to the lower reactor vessel head.

Measurements were also performed on the individual debris samples from Particle 11-5-C for gamma ray emitters, I-129, Sr-90, and fissile material content. Two radionuclides of primary interest are Cs-137 and I-129. Analysis results for these radionuclides are listed in Table 4. Also, the ratio is listed for the measured to expected concentrations of both radionuclides. These data indicate a corresponding change in concentration for both radionuclides as a function of position in the sample. The retention data indicate the radionuclides are not retained to the same extent in the debris, i.e., the Cs-137 is retained from 7.6 to 14.9 times more than the I-129 as a fraction of core inventory. Although the concentrations of both radionuclides are generally higher in the area of higher porosity, the degree of porosity and fission product retention has not been determined to be related. The samples will be analyzed in more detail to evaluate potential mechanisms for retaining Cs-137 and I-129 in the debris.

Table 5 shows a comparison of measured fission product retentions in the upper and lower debris beds. The measured radionuclides are listed in the order of their expected volatilities, with the most volatile listed first. Note these retention data are based on small samples (0.01 to 50 gm) and may not be generally representative of either the upper or lower plenum debris. The trend of the data is consistent with the expected volatilities of the fission products with a few exceptions (particularly Cs-137, Sb-125, and Ru-106, which are discussed in detail). A comparison of the I-129 retention data for the upper and lower debris beds indicates substantially greater retention in the upper debris bed. The higher retention probably occurs because the upper debris bed samples are composites of relatively intact fractured fuel material and prior

TABLE 2. AVERAGE ELEMENTAL COMPOSITION[a]

Element	Core Average (wt %)	Particle 11-5-C (wt %)
U	71.8	62.9
Zr	19.9	11.8
Fe	3.0	2.0
Cr	1.0	0.6
Ni	0.9	0.2
Cd	0.12	0.3
Mn	0.09	0.06

a. As determined from inductively coupled plasma spectroscopy analysis.

TABLE 3. LOWER VESSEL DEBRIS URANIUM CONTENT

Sample	Uranium Content (wt %)[a] Average	Range
7-1-B	68	62-70
11-2-C	68	63-78
11-4-B	63	58-72
11-4-D	66	62-69
11-6-B	65	62-68
11-7-C	59	43-71

a. As determined from neutron activation analysis and subsequent delayed neutron counting.

TABLE 4. CESIUM AND IODINE CONCENTRATIONS IN PARTICLE 11-5-C

Sample Location	^{129}I (μCi/gm)	^{137}Cs (μCi/gm)	Ratio Fraction of Core Inventory[a]
1	<8.2E-6	2.55E+1	--
2	<2.0E-6	6.75E+1	--
3	2.38E-6	1.12E+2	14.9
4	7.72E-6	2.36E+2	9.6
5	--[b]	4.36E+2	--
6	3.03E-5	7.29E+2	7.6
7	2.89E-5	8.63E+2	9.4
8	3.15E-5	1.03E+3	10.3
9	2.15E-5	9.27E+2	13.6

a. Ratio of fission product retentions as fractions of core inventory.

b. No sample.

TABLE 5. AVERAGE RADIONUCLIDE RETENTION IN UPPER AND LOWER VESSEL DEBRIS BEDS

	Percent of Inventory Retained[a]			
	Lower Plenum		Upper Debris	
Radionuclide	Average	Range	Average	Range
^{129}I[b]	2	0-10	22	10-28
^{137}Cs	16	9-22	21	6-32
^{125}Sb	5	3-10	28	18-38
^{106}Ru	7	4-9	55	35-86
^{144}Ce	114	106-124	114	90-130
^{154}Eu	85	75-94	90	60-108

a. Compared with whole core average ORIGEN-2 analysis (μCi/gU) and average uranium content.

b. Average radionuclide content based on average of number of small (5 to 40 mg) particle analyses.

molten fuel whereas the lower debris bed is composed of prior molten ceramic material, and consequently, had a greater release of available iodine.

A comparison of the Cs-137 data in Table 5 indicates similar retention in both the upper and lower vessel debris. This is important because the lower vessel debris is principally composed of prior molten material which would be expected to release all cesium during the high temperature portion of the accident. As previously discussed, the autoradiography data provide inferential evidence the retained cesium may be trapped on the surfaces of the void spaces and at grain boundaries in the debris.

The Sb-125 results indicate significantly lower retentions in both the upper and lower debris beds than would be anticipated based on the expected relative volatility (medium) of this fission product. In the upper debris bed, the retentions indicate significant release of this radionuclide; however, some of the analytical results provide a possible explanation for the apparent relocation of this fission product. Analysis of samples containing little or no fuel material from the upper core[2] indicates significant retention of antimony in or on non-fuel material, probably as surface deposited species. Also, in two instances, an apparent scavenging effect by non-fuel particles was observed in which large concentrations of both Sb-125 and Ru-106 were observed in conjunction with non-fuel material, particularly material containing nickel. Reference 3 suggests antimony has a relatively high oxygen potential and probably remains as a metallic rather than an oxide. These data, although based on only a few samples, suggest the relocated Sb-125 has either been deposited on surfaces in the vessel and upper plenum or has been scavenged as a metal by liquefied structural material and deposited in accumulations in the core.

The Ru-106 results listed in Table 5 also indicate significant depletion of this radionuclide. This fission product has two relatively volatile oxides (RuO_2 and RuO_4) which display significant mobility; however, these form only at a high oxygen potential, and the ruthenium at TMI-2 is expected to be retained as a metal. As discussed above, the analytical results indicate scavenging of this radionuclide and probable relocation into lower portions of the core as metallic nodules.

The lanthanide results (Ce-144 and Eu-154) indicate complete, or nearly complete, retention for both radionuclides in the debris. The >100% retentions listed for Ce-144 and the >100% retentions listed for Eu-154 probably result from (a) concentration comparisons that are made with core average fission product concentrations, (b) uncertainties (up to 30% for some radionuclides) in the ORIGEN-2 Code , and (c) samples from areas that may contain greater than average burnup.

SUMMARY OF RESULTS

The results of the lower vessel debris examinations are preliminary as all analyses have not been completed yet. Also, additional data are expected to be received from samples from other portions of the core that may change the observations made concerning fission product behavior based on currently available results. The principal observations and results of the examinations performed to date are as follows:

1. Oxidized chromium and iron are found in the grain boundaries in a fine dendritic structure.

2. Metallic inclusions in the fuel are mixtures of nickel and tin, nickel and silver, and nickel and ruthenium. Some isolated particles of silver were found in the pores.

3. Debris in the lower head are a mixture of stoichiometric uranium and zirconium oxides.

4. Substantial amounts of Cs-137 are retained in the lower reactor vessel debris.

5. Elements Sb-125 and Ru-106 are retained to some extent in the debris, probably as metallic nodules.

6. Lanthanides are retained almost entirely in the fuel material and are not released to the reactor coolant system.

REFERENCES

1. J. M. Broughton, "Core Condition and Accident Scenario", Proceedings of the First International Meeting on the TMI-2 Accident CONF-8510166 (October 1985).

2. D. W. Akers et al., TMI-2 Core Debris Grab Samples--Examination and Analysis, GEND-INF-075, September 1986.

3. R. R. Hobbins et al., "Insights on Severe Accident Chemistry from TMI-2," Symposium on Chemical Phenomena Associated with Radioactivity Releases During Severe Nuclear Plant Accidents, September 10-14, 1986.